

# Optimization of Tooth Surface Modification for High-Speed Helical Face Gear Transmission Based on Meshing Impact

Xuezhong Fu <sup>\*</sup>, Yujian Yan <sup>a</sup>, Xudong Liu <sup>b</sup>, Gaoming Zhou <sup>c</sup>

Guangxi University of Science and Technology, Liuzhou, China

\* Corresponding Author Email: fxznwpu@163.com, <sup>a</sup>20240102041@stdmail.gxust.edu.cn, <sup>b</sup>m15822067414@163.com, <sup>c</sup>202100107182@stdmail.gxust.edu.cn

**Abstract.** In order to reduce the influence of meshing impact on high-speed helical face gear transmission, the expression of meshing impact force of helical face gear is derived, and the modification curve of pinion composed of parabola at both ends and a straight line is designed. An optimization model of tooth surface modification of high-speed helical face gear transmission is established, which takes the modification parameters as the optimization variables and the minimum relative speed of meshing impact as the objective. The influence of input speed and load on meshing impact of helical face gear is analyzed. The results show that when the speed of the pinion is 10000r/min and the working load is 500N·m, the reduction amplitude of the meshing impact force reaches 44.75% by optimizing the modification curve parameters of the pinion tooth surface, which effectively reduces the meshing impact force of the helical face gear pair at high speed.

**Keywords:** helical face gear, meshing impact, tooth surface modification, optimization.

## 1. Introduction

Helical face gear transmission is an advanced new type of gear transmission with helical cylindrical gear and bevel gear meshing [1], which can be used in the case of two gears axes intersecting or interleaving. Helical face gears have unique shunt characteristics. At present, they are mainly used in high-speed and heavy-duty occasions such as the main reduction and split torque system in heavy-duty helicopters (such as Apache AH-64) in the aviation field [2] and the central differential in high-performance vehicles [3]. At present, the research on the modification of helical face gear at home and abroad mostly focuses on the tooth profile modification of face gear [4-8], the 3D modification of face gear vibration [9], the modification of pinion tooth surface [10-12], etc. The research on meshing impact has the load behavior of face gear meshing impact [13], the influence of machining error and elastic deformation of face gear on meshing impact [14], the alternating meshing characteristics of face gear meshing impact [15]. Although the research in the above literature has been designed to optimize the modification of the gear tooth surface, there is no research on the modification of the tooth surface of the high-speed helical gear transmission considering the meshing impact.

Both the test and the standard indicate that higher rotational speeds lead to greater dynamic responses of the gear. However, the load transmission error is the primary vibration excitation in the speed domain below the resonance region. Once the rotational speed enters the super-resonance region, the load transmission error no longer exerts a significant excitation effect. In this region, meshing impact can be considered the dominant vibration excitation for high-speed gears. As mentioned above, the rotational speed of the aviation face gear exceeds 20,000r/min, indicating that the super-resonance region has been reached. Therefore, researching tooth surface modification optimization for high-speed helical face gear transmissions based on meshing impact is of great significance. However, there is limited literature available, both domestically and internationally, on the study of tooth surface modification in high-speed helical gear transmissions considering meshing impact.

This paper derives the expression for the meshing impact force of the helical face gear and establishes an optimization model for tooth surface modification of high-speed helical face gear transmissions. The model uses modification parameters as optimization variables, with the goal of minimizing the relative speed of meshing impact. This provides a reference for reducing meshing impact and enhancing the performance of high-speed helical face gear pairs.

## 2. Meshing impact calculation of helical face gear transmission

### 2.1. Determination of the Position of the Initial Meshing Point

Meshing impact includes meshing in and meshing out impact, but meshing in impact is the main excitation of gear vibration. The key to calculate the meshing impact is to determine the meshing point. In the meshing process of the helical face gear pair, it is similar to the meshing of the helical cylindrical gear. Therefore, the basic principle of the meshing impact of the helical face gear is similar to that of the helical cylindrical gear. The basic principle is shown in Fig. 1 ( where Pinion 1 is the driving gear, Gear 2 is the driven gear, and  $\varphi_1$  represents the engagement angle of the pinion).

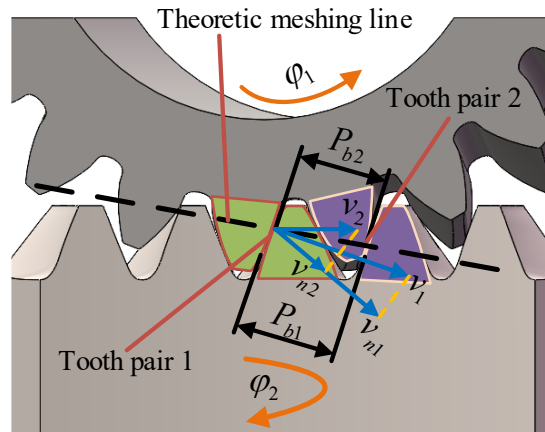


**Figure 1.** Schematic diagram of meshing impact

The location of the impact point is determined by TCA technology and LTCA technology. As shown in Fig. 2, the theoretical meshing point position analysis diagram is shown.  $T_E$  is the transmission error curve, curve 1 is the geometric transmission error, and curve 2 is the bearing transmission error. At the meshing position,  $\delta$  is the value of the bearing transmission error,  $\delta_1$  is the transmission error of the first pair of meshing gear teeth at this time, and  $\delta_2$  is the angle value of the passive gear relative to the theoretical meshing position in the meshing process.

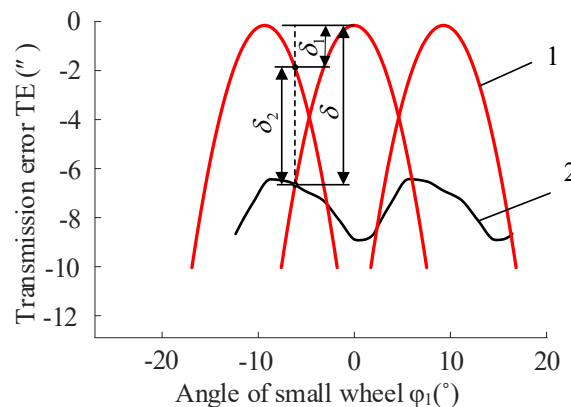


**Figure 2.** Schematic diagram of theoretical meshing point position analysis

### 2.2. Calculation of Impact Velocity

In the helical face gear transmission, when the tooth surface is subjected to the load, the tooth base of the large and small gears changes, resulting in a deviation between the actual contact point and the theoretical contact line. The error of the gear surface will also cause the above deviation. Due to the existence of these variables, the gear pair of the initial meshing point has inconsistent speed of the contact point. The speed difference is called the meshing impact speed, which is quantified according to the geometric relationship shown in Fig. 1. The calculation expression of impact velocity is as follows:

$$\begin{cases} \mathbf{v}_1 = \boldsymbol{\omega}_1 \times \mathbf{r}_h \\ \mathbf{v}_2 = \boldsymbol{\omega}_2 \times \mathbf{r}_h \\ \mathbf{v}_s = (\mathbf{v}_1 - \mathbf{v}_2) \mathbf{n}_h \end{cases} \quad (1)$$

In the formula,  $v_1$  and  $v_2$  are the linear velocities of the pinion and face gear at the initial meshing point;  $\mathbf{n}_h$  is the normal vector at the initial meshing point of the tooth surface in the common meshing coordinate system;  $\omega_1$  and  $\omega_2$  are the rotational speeds of the pinion and face gear, respectively; and  $r_h$  is the position vector of the initial meshing point in the common meshing coordinate system.

### 2.3. Calculation of Impact Force

Under actual working conditions, due to the existence of impact velocity, the helical face gear will produce impact force at the initial meshing point. The magnitude and variation of impact force are closely related to impact velocity and single tooth meshing stiffness. The impact force  $F_s$  at the initial meshing point is calculated according to the following formula:

$$\begin{cases} J_1 = \frac{\pi \rho b}{2} (r_{b1}^4 - r_{h1}^4) \\ J_2 = \frac{\pi \rho b}{2} (r_{b2}^4 - r_{h2}^4) \\ E_k = \frac{1}{2} \frac{J_1 J_2}{J_1 r_{b2}^2 + J_2 r_{b1}^2} v_s^2 \\ \delta_s = \left( \frac{n+1}{2} \frac{J_1 J_2}{(J_1 r_{b2}^2 + J_2 r_{b1}^2) k_s} (v_s)^2 \right)^{\frac{1}{n+1}} \\ F_s = \left( \frac{n+1}{2} \frac{J_1 J_2}{J_1 r_{b2}^2 + J_2 r_{b1}^2} v_s^2 K_s^{1/n} \right)^{\frac{n}{n+1}} \end{cases} \quad (2)$$

In the formula,  $b$  is the tooth width;  $\rho$  is the material density;  $r_{h1}$  and  $r_{h2}$  are the inner hole radius of the hub of the small wheel and the large wheel respectively;  $r_{b1}$  and  $r_{b2}$  are the base circle radius of the small wheel and the large wheel entering the meshing instant, respectively.  $J_1$  and  $J_2$  are the moment of inertia of the small wheel and the moment of inertia of the big wheel respectively;  $E_k$  is the impact kinetic energy at the initial meshing point;  $\delta_s$  is the normal deformation of tooth surface.

## 3. Tooth surface modification design of pinion

### 3.1. Small Wheel Modification Curve Design

Fig. 3 shows the modification curve of the pinion design. The  $l_1$  and  $l_3$  in the tooth profile modification curve are the maximum modification amount on both sides, and  $l_2$  and  $l_4$  are the corresponding modification length. The  $l_5$  and  $l_7$  in the tooth profile modification curve are the maximum modification amount on both sides, and  $l_6$  and  $l_8$  are the corresponding modification length.  $r_a$  and  $r_h$  are the addendum height and root height on the rotating projection surface respectively, and  $b$  is the tooth width of the pinion.

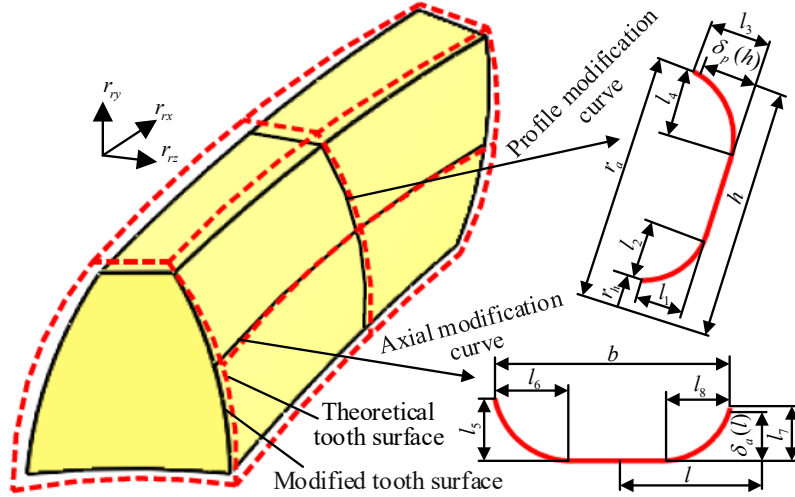


**Figure 3.** Small wheel modification curve

In the process of generating the theoretical tooth surface of the pinion, the definition vector  $R_r(u_1, l_1)$  is controlled by two independent variables  $u_1$  and  $l_1$ . The three coordinate components of the position vector  $R_r(u_1, l_1)$  are  $R_{rx}(u_1, l_1)$ ,  $R_{ry}(u_1, l_1)$ ,  $R_{rz}(u_1, l_1)$ . When these coordinates are converted to the rotating projection plane, their positions can be expressed by the functions of  $h$  and  $l$ :

$$\begin{cases} h = \left[ R_{rx}^2(u_1, l_1) + R_{ry}^2(u_1, l_1) \right]^{1/2} \\ l = R_{rz} \end{cases} \quad (3)$$

When  $k$  is used to represent the number of parabolic segments of the modification curve ( $k$  usually takes 2, 4 and other even numbers, 2 is selected in this paper), the representation of the tooth profile modification curve  $\delta_p(h)$  and the tooth profile modification curve  $\delta_a(l)$  is shown in Reference [16].

### 3.2. Pinion Modified Tooth Surface

At the position of  $(h, l)$ , the modification amount  $\delta(h, l)$  of the pinion can be expressed as the sum of the profile modification amount  $\delta_p(h)$  and the axial modification amount  $\delta_a(l)$ , namely:

$$\delta(h, l) = \delta_p(h) + \delta_a(l) \quad (4)$$

By superimposing the theoretical tooth surface  $R_r(u_1, l_1)$  of the pinion with the modified surface, the topological modified tooth surface of the pinion can be obtained. The potential vector and normal vector of the tooth surface are shown in Reference [16].

## 4. Establishment of optimization model and optimization algorithm

### 4.1. Optimization Model

According to the above calculation, the meshing impact force is affected by the relative velocity and meshing stiffness. In order to facilitate the optimization calculation, this paper optimizes the meshing impact by optimizing the minimum relative speed, so as to effectively reduce the meshing impact.

Optimization variables:  $l_1, l_2, l_3, l_4, l_5, l_6, l_7, l_8$

Objective function:

$$\min f = |v^{12}| \quad (5)$$

Objective function:

$$\text{s.t.} \begin{cases} \delta_{\min}^p \leq l_1, l_3 \leq \delta_{\max}^p \\ l_{\min}^p \leq l_2, l_4 \leq l_{\max}^p \\ \delta_{\min}^a \leq l_5, l_7 \leq \delta_{\max}^a \\ l_{\min}^a \leq l_6, l_8 \leq l_{\max}^a \end{cases} \quad (6)$$

## 4.2. Optimistic Algorithm

In this paper, genetic algorithm is used to optimize the design. Genetic algorithm parameter settings: the population size is 20, the evolution termination algebra is 60, the mutation probability is 0.05, and the crossover probability is 0.9. According to the above meshing impact analysis, the self-written program is used to solve the optimization model equations (5) and (6) by genetic algorithm. Fig. 4 shows the specific optimization process.

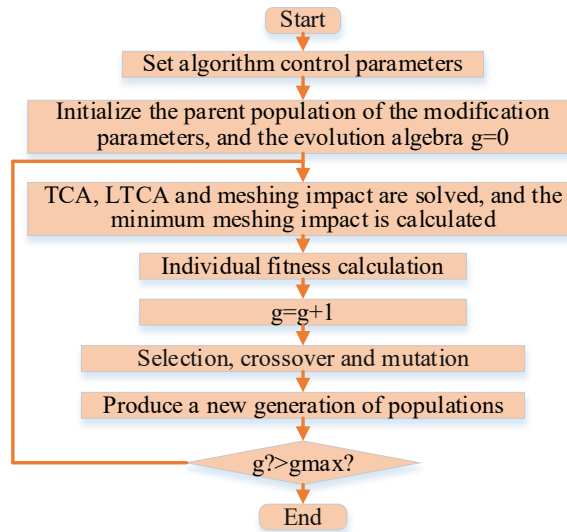


Figure 4. Optimization process of tooth surface modification

## 5. Examples and Analysis

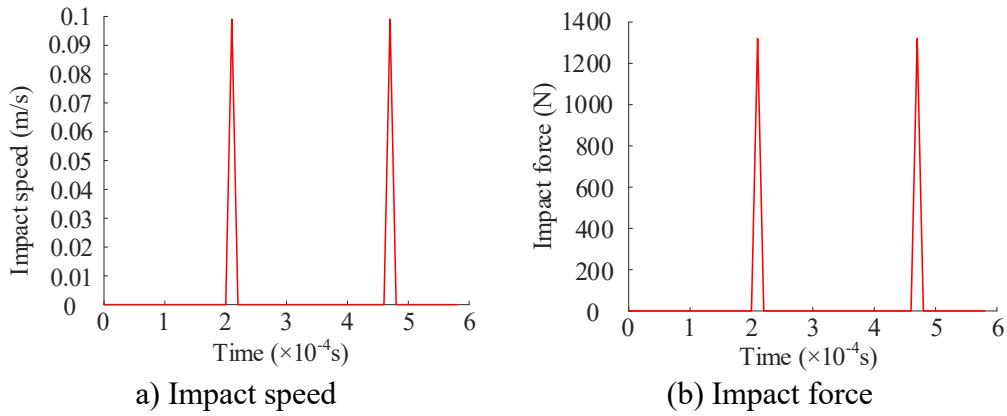
In this paper, the parameters of the helical face gear pair, as presented in Tab. 1, are used as an example to analyze the meshing impact. The input speed of the gear pair is  $S_p = 10000 \text{ r/min}$ , and the load is  $T_N = 500 \text{ N}\cdot\text{m}$ . According to the LTCA method, the normal deformation  $\delta_s$ , the load distribution coefficient  $k_a$  and the total normal force  $P$  of the helical gear at the initial meshing point of the tooth surface under the given load are calculated. The meshing impact velocity and impact force of helical face gear under given working conditions are calculated by formula (1) and formula (2). The calculation results are shown in Tab. 2 and Fig. 5.

Table 1. Input Parameters

Parameter Name	Parameter Value	Parameter Name	Parameter Value
Number of teeth on gear shaper cutter $N_s$	28	Face gear teeth $N_2$	120
Normal surface pressure $\alpha_n(^{\circ})$	20	Helix angle $\beta(^{\circ})$	10
Normal face mold $m_n(\text{mm})$	4	axes-angle $\gamma_m(^{\circ})$	90

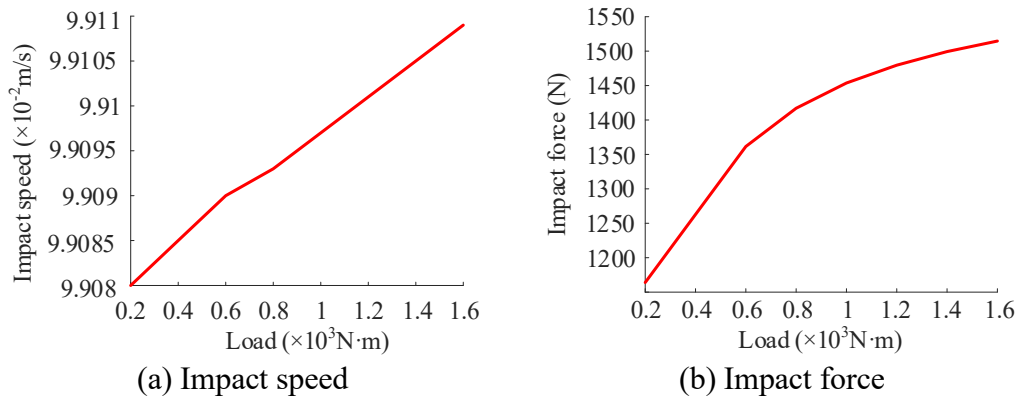
Table 2. Meshing impact

Item	Value
Stiffness of Single Tooth Meshing (N/m)	$0.7915 \times 10^8$
Meshing Force Index	1.1
Impact speed (m/s)	0.0991
Impact force (N)	1320.29



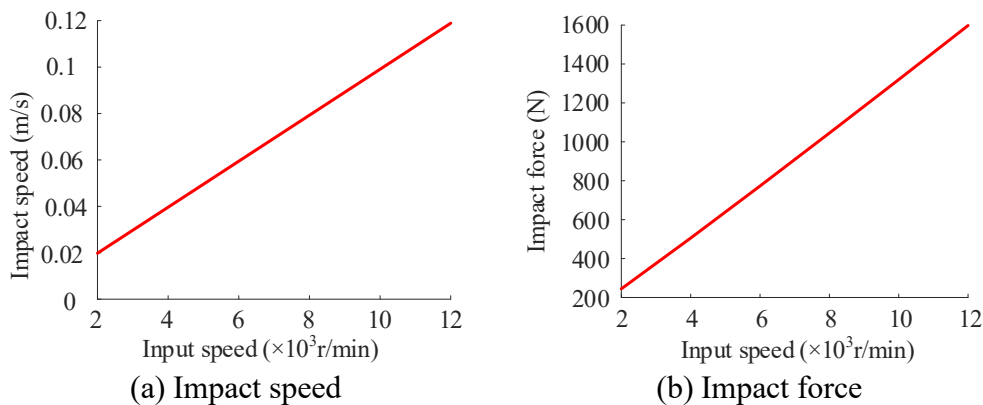
**Figure 5.** Meshing impact of helical face gear pairs under given working conditions

Fig. 6 shows that when the input speed is constant, the load is increased from 200N·m to 1600N·m according to the given step size, and the variation of the meshing impact of the initial meshing point on the tooth surface of the gear pair with the load is calculated



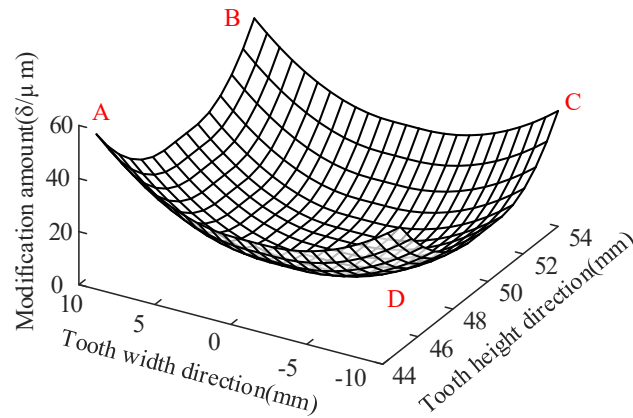
**Figure 6.** The variation law of meshing impact with load

Fig. 7 shows the gradual increase of the gear's input speed from 2000r/min to 12,000r/min under a load of 500N·m. Using formulas (1) and (2), the impact velocity and impact force of the gear pair at different input speeds are calculated and presented in the diagram. Through analysis and comparison, it can be observed that as the input speed increases, the impact velocity also increases, leading to a corresponding rise in impact force.



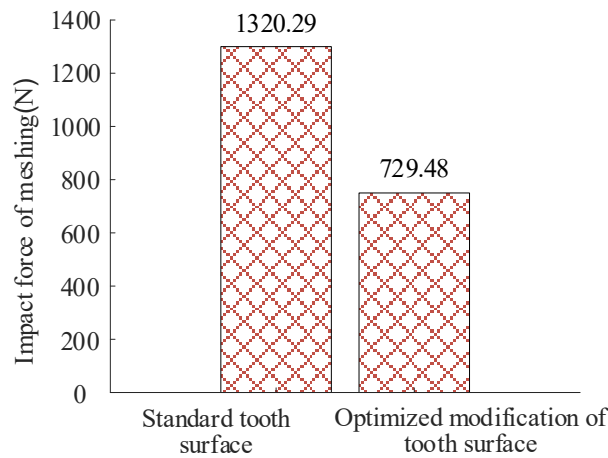
**Figure 7.** The variation law of helical face gear pair meshing impact with input speed

Fig. 8 shows the optimized modified surface. The modification amounts at the vertices A, B, C, and D of the modified surface are 51.46 $\mu$ m, 48.42 $\mu$ m, 43.51 $\mu$ m, and 46.55 $\mu$ m, respectively. Modification curve parameters:  $l_1 = 26.21\mu\text{m}$ ,  $l_2 = 3.98\text{mm}$ ,  $l_3 = 23.17\mu\text{m}$ ,  $l_4 = 3.29\text{mm}$ ,  $l_5 = 20.34\mu\text{m}$ ,  $l_6 = 8.88\text{mm}$ ,  $l_7 = 25.25\mu\text{m}$ ,  $l_8 = 9.06\text{mm}$ .



**Figure 8.** Reducing mesh impact and modifying curved surface

As shown in Fig. 9, the comparison of meshing impact force before and after tooth surface modification is presented under the condition of a pinion speed of 10,000r/min. The diagram illustrates that the meshing impact force without modification is 1320.29N, while after optimization, it is reduced to 729.48N, representing a 44.75% decrease. This clearly demonstrates the effectiveness of the tooth surface optimization in reducing the meshing impact force. When the standard tooth surface engages, the teeth deform under load, leading to meshing interference and a larger impact force. After modification, the clearance between the teeth is increased, compensating for the deformation caused by the load. This effectively eliminates meshing interference, resulting in a significant reduction in impact force.



**Figure 9.** Comparison of meshing impact force before and after tooth surface modification

## 6. Conclusion

(1) An increase in input speed leads to a corresponding rise in both meshing impact speed and impact force. Calculation results indicate that the effect of input speed on meshing impact is more significant than that of the load.

(2) Taking the pinion as the modification object, a modification curve consisting of parabolic sections at both ends and a straight line is designed. This curve allows for precise and direct control over the amount, length, and surface of the modification.

(3) By optimizing the modification of the pinion tooth surface, the reduction in meshing impact force reaches 44.75%, effectively decreasing the meshing impact force of the helical gear pair at high speeds and enhancing the performance of the high-speed helical gear transmission.

## Acknowledgment

This work was financially supported by the Guangxi Natural Science Foundation (No. 2022GXNSFBA035574), and the National College Students Innovation and Entrepreneurship Training Program Funding Project (No.202310594035).

## References

- [1] F. L. Litvin, A. Egelja, J. Tan, D. Chen, and G. Heath, "Handbook on face gear drives with a spur involute pinion", Technical Report No. CR - 2000 - 209909, 2000.
- [2] G. F. Heath, S. C. Slaughter, D. J. Fisher, D. G. Lewicki, and J. Fetty, "Helical face gear development under the enhanced rotorcraft drive system program," In 67th Annual Forum and Technology Display (Forum 67), AHS 2011 - 000270. 2011.
- [3] A. Benz, "Cylkro® face gears: Dutch design and Swiss ingenuity cause transmission breakthrough," International Gear Conference 2014, pp. 1184 - 1187, August 2014.
- [4] F. L. Litvin, A. Fuentes, and M. Howkins, "Design, generation and TCA of new type of asymmetric face-gear drive with modified geometry," Computer methods in applied mechanics and engineering, vol. 190, no. 43 - 44, pp. 5837 - 5865, 2001.
- [5] M. Tsay, and Z. Fong, "Novel profile modification methodology for moulded face-gear drives," Proceedings of the Institution of Mechanical Engineers, Part C: Journal of Mechanical Engineering Science, vol. 221, no. 6, pp. 715 - 725, 2007.
- [6] T. Inoue, and S. Kurokawa, "Derivation of path of contact and tooth flank modification by minimizing transmission error on face gear," Journal of Advanced Mechanical Design, Systems, and Manufacturing, vol. 6, no. 1, pp. 15 - 22, 2012.
- [7] Y. B. Shen, Z. D. Fang, N. Zhao, and H. Guo, "Meshing Performance of Modified Face Gear Drive with Helical Pinion in the Profile Direction," Journal of Mechanical of Engineering, vol. 19, no. 18, pp. 2219 - 2222, 2008.
- [8] C. Jia, B. Li, and J. Xu, "A Novel Tooth Modification Methodology for Improving the Load-Bearing Capacity of Non-Orthogonal Helical Face Gears," Machines, vol. 11, no. 12, pp. 1077, 2023.
- [9] C. Wang, "Study on 3-D modification for reducing vibration of helical gear based on TCA technology, LTCA technology and system dynamics," Mechanical Systems and Signal Processing, vol. 146, pp. 106991, 2021.
- [10] C. Zanzi, and J. I. Pedrero, "Application of modified geometry of face gear drive," Computer Methods in Applied Mechanics and Engineering, vol. 194, no. 27 - 29, pp. 3047 - 3066, 2005.
- [11] S. Barone, L. Borgianni, and P. Forte, "Evaluation of the effect of misalignment and profile modification in face gear drive by a finite element meshing simulation," J. Mech. Des., vol. 126, no. 5, pp. 916 - 924, 2004.
- [12] X. Z. Fu, Z. D. Fang, Y. B. Guan, and J. H. Li, "NSGA-II based multi-objective optimization on topologically modified pinions for face gear pairs," Journal of Xi 'an Jiaotong University, vol. 51, no. 7, pp. 98 - 104, 2017.
- [13] R. P. Shao, J. C. Sun, Y. W. Shen, and P.R. Jia, "Quantitative prediction of gear meshing impact noise," mechanical science and technology, vol. 20, no. 3, pp. 340 - 342, 2001.
- [14] M. Guingand, J. P. de Vaujany, and Y. Icard, "Analysis and optimization of the loaded meshing of face gears," J. Mech. Des., vol. 127, no. 1, pp. 135 - 143, 2005.
- [15] Y. Kang and Z. Y. Shi, "Sequential Analysis and Evaluation Method of Gear Impacts," Journal of Tianjin University: Science and Technology, vol. 46, no. 5, pp. 440 - 447, 2013.
- [16] X. Z. Fu, Z. D. Fang, X. L. Peng, X. Y. Hou, and J. H. Li, "Computerized Design and Optimization of Tooth Modifications on Pinions for Face Gear Drives," Arabian Journal for Science and Engineering, vol. 44, no. 2, pp. 1097 - 1108, 2018.